

Chapter 4

CERN–ELIN Nb₃Sn Dipole Model



Romeo Perin

Abstract This chapter reports on the European Organization for Nuclear Research (CERN)–ELIN Nb₃Sn dipole program. In this program a 1 m long model magnet was built, using Nb₃Sn superconductor. The Nb₃Sn magnet reached field levels of 9.5 T in the full dipole and 10.2 T in the magnetic mirror configuration in a 50 mm bore.

4.1 Introduction

In the second half of the 1980s, in the initial phase of the development of the magnets for the Large Hadron Collider (LHC), a crucial issue was the choice of the superconductor. The only industrially available materials at that time were Nb–Ti and Nb₃Sn. The former had already been successfully used in large solenoids such as the OMEGA (Morpurgo 1970) and the Big European Bubble Chamber (BEB) magnets (Haebel and Wittgenstein 1971), in the Intersecting Storage Rings (ISR) superconducting quadrupoles (Billan et al. 1976) at the European Organization for Nuclear Research (CERN), and then massively in the Tevatron (Wilson 1978) and Hadron-Elektron-Ring-Anlage (HERA) (Wolff 1988) particle accelerators. Nevertheless, the field level required for the LHC, between 8 and 10 T, could be reached only by lowering the operating temperature to about 1.9 K, requiring a new cryogenic system, still to be developed.

At that time, Nb₃Sn had been used only in a few short model magnets, with mixed success. Its brittleness forbids winding reacted conductor around small curvature radii (about 5 mm for the LHC dipole coils) and, thus obliges that coils are wound with conductors containing precursors of the superconducting compound. The wound coil then has to be submitted to a heat treatment at about 700 °C to form the superconducting phase. This heat treatment step at about 700 °C required the development and use of insulation systems able to withstand this treatment, the construction of a complex tooling to maintain the coil strongly confined in its precise

R. Perin (✉)

CERN (European Organization for Nuclear Research), Meyrin, Genève, Switzerland

e-mail: romeo.perin@cern.ch

© The Author(s) 2019

D. Schoerling, A. V. Zlobin (eds.), *Nb₃Sn Accelerator Magnets*, Particle Acceleration and Detection, https://doi.org/10.1007/978-3-030-16118-7_4

87

shape during the whole fabrication process, and extreme care in all handling operations after the reaction heat treatment to not damage the brittle superconductor.

In view of the considerable potential of Nb₃Sn, notably its high critical current density at the field levels required at 4.2 K, and the higher specific heat and temperature margins as compared to Nb-Ti at 1.9 K, CERN decided to build a 1 m long dipole model using this superconductor. This decision was taken to ensure that the best choice for the LHC would be adopted, although the construction of this Nb₃Sn dipole model came with numerous challenges, which had to be overcome. An additional argument to test Nb₃Sn technology was the potential need for high-strength quadrupoles in the interaction regions with large apertures and in the presence of increased heat and radiation load.

The strategy for the construction of the Nb₃Sn dipole magnet was like that adopted for a Nb-Ti model (Perin et al. 1989), i.e., to design and build the magnet in close collaboration with a qualified industrial partner (Perin 1990). The reason for this approach was twofold: (1) to involve industry in the technological development in order to prepare it for the future production of the LHC magnets; and (2) the clearly insufficient resources available at that time in the CERN laboratory for LHC magnet research and development (R&D), as CERN was heavily committed to the construction of the Large Electron–Positron Collider (LEP).

A CERN delegation paid visits to several European electromechanical companies to invite them to collaborate with CERN in the development of the LHC magnets. Thorough discussions took place with the firms that expressed an interest: ELIN-UNION at Weiz, Austria, was selected as the most suitable for building a short model magnet using Nb₃Sn superconductor.

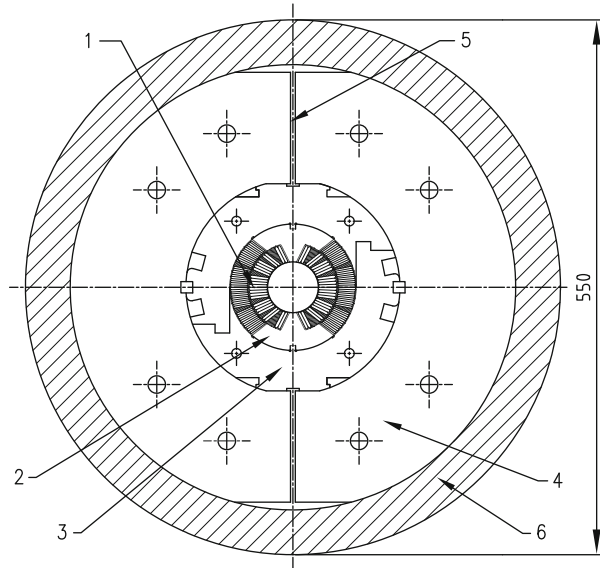
4.2 The CERN–ELIN Collaboration Agreement

A Collaboration Agreement for the design, manufacture, and testing of a 50 mm aperture, 1 m long single bore dipole model magnet using Nb₃Sn conductor was signed in August 1986 with the Austrian company ELIN-UNION.

In summary, the agreement foresaw the following.

- The design of the magnet and all necessary tooling were to be done at CERN by a common CERN–ELIN team. For this purpose, ELIN, at its own cost, sent to CERN one graduate electromechanical engineer, one production engineer, and one designer, who were integrated into the CERN project team.
- The superconducting cable was specified, procured, and qualified by CERN and then supplied to ELIN.
- Manufacturing of tooling, coils, mechanical parts, test assemblies, final assembly of the magnet, and factory tests were ELIN's responsibility with the assistance of members of the CERN team in the most delicate phases.
- Final tests were made at the CERN cryogenic laboratory under CERN's responsibility with the assistance of members of the ELIN team.
- The dipole magnet remains the property of ELIN.

Fig. 4.1 Simplified cross-section of the magnet: 1 – coil; 2 – coil central post; 3 – collar; 4 – iron yoke; 5 – gap; 6 – shrinking cylinder



After the successful conclusion of this project and CERN's decision to adopt the Nb-Ti line for the LHC magnets, the collaboration of CERN with ELIN continued with the construction of short and long Nb-Ti models until the end of 1994.

4.3 Magnet Design Concept

The design, construction, and performance of the Nb₃Sn 1 m long model magnet are described in Wenger et al. (1989) and Asner et al. (1990). Transverse dimensions, coil cross-section, and the magnetic and mechanical structures were designed to be compatible with the 1985 preliminary design of the two-in-one dipole magnet for the LHC (Hagedorn et al. 1985). A simplified cross-section of the dipole cold mass is shown in Fig. 4.1. The main components are the two layer coils, a set of aluminum alloy (Al-Mg-4.5Mn) collars locked by stainless-steel keys, a laminated iron yoke vertically split in two halves, and an outer aluminum alloy (Al-Mg-4.5Mn) shrinking cylinder. The main parameters of the magnet are summarized in Table 4.1.

4.4 Superconducting Strands and Cables

Each coil consists of two layers composed of insulated Nb₃Sn Rutherford-type, keystone cables having the same width but different thickness to grade the current density to peak field in each of the two layers. The superconducting cables were made from multifilamentary bronze route Nb₃Sn wires: their characteristics are

Table 4.1 Parameters of the magnet

| Parameter | Value |
|--|-------|
| Coil aperture diameter (mm) | 50 |
| Shrinking cylinder outer diameter (mm) | 550 |
| Magnetic length (m) | ~1 |
| Overall length (m) | ~1.4 |
| Overall mass (kg) | ~2000 |
| Nominal central field (T) | 10 |
| Peak field in inner layer cable (T) | ~10.5 |
| Nominal current I_{nom} (kA) | 16.3 |
| Stored energy at I_{nom} (kJ) | 360 |
| Lorentz forces F_x on first coil quadrant (MN/m) | 2.3 |
| Lorentz forces F_y on first coil quadrant (MN/m) | -1.2 |
| Axial Lorentz force F_z per magnet end (MN) | 0.32 |

Table 4.2 Characteristics of the superconducting cables

| Parameter | Inner layer | | Outer layer | |
|--|-----------------------------|-----------|-------------|-----------|
| | Bronze | PIT | Bronze | PIT |
| Cable width (mm) | 16.81 | 16.40 | 16.81 | 16.40 |
| Cable thickness min/max (mm) | 2.19/2.69 | 2.40/2.70 | 1.47/1.79 | 1.45/1.77 |
| Strand diameter (mm) | 1.38 | 1.37 | 0.92 | 0.90 |
| Cu/non-Cu ratio | 0.38 (0.22 ^a) | 0.55 | 0.36 | 0.55 |
| Strand number | 24 | 24 | 36 | 36 |
| Filament number | 50,000 | 192 | 20,000 | 192 |
| Nb ₃ Sn filament diameter (μm) | 2.6 | 47 | 2.6 | 33 |
| $I_c(11\text{ T}, 4.2\text{ K})$ (kA) | ~18.1 (~19.6 ^a) | ~23 | ~11.6 | ~16.5 |
| $I_c(12\text{ T}, 4.2\text{ K})$ (kA) | ~16.4 (~17 ^a) | ~17.5 | ~10 | ~13.5 |

^aThese values pertain to the “mirror” coil inner layer. PIT powder-in-tube

reported in Table 4.2. These wires and cables (bronze route) were produced by Vacuumschmelze GmbH, Germany.

Cross-sections of inner and outer coil layer cables are shown in Figs. 4.2 and 4.3. A thin tantalum diffusion barrier (about 4% of the strand cross-section) separates the bronze/Nb/Nb₃Sn part from the outer stabilizing copper ring.

Samples, some of which were bent around a 5.5 mm radius before reaction, and a cable-to-cable splice about 125 mm long, were measured at the Fermi National Accelerator Laboratory (FNAL), which was at that time the only place having a suitable test station. No sample could be quenched up to 10.8 T and 19.7 kA at 4.2 K. The contact resistance of the splice measured at this field and current was about 1.25 n Ω .

An early coil (mirror coil), tested in the Mirror Coil Test Facility (see Sect. 4.7), had an inner shell made with a higher Nb₃Sn content cable (Cu/non-Cu ratio of 0.22 instead of 0.38).

Cable $I_c(B)$ lines and calculated coil load lines are shown in Fig. 4.4. The cable $I_c(B)$ lines were defined by adding the measured I_c of reacted round strands (not

Fig. 4.2 The inner layer cable's narrow edge showing strongly deformed strands. (Courtesy of Vacuumschmelze GmbH, Germany)

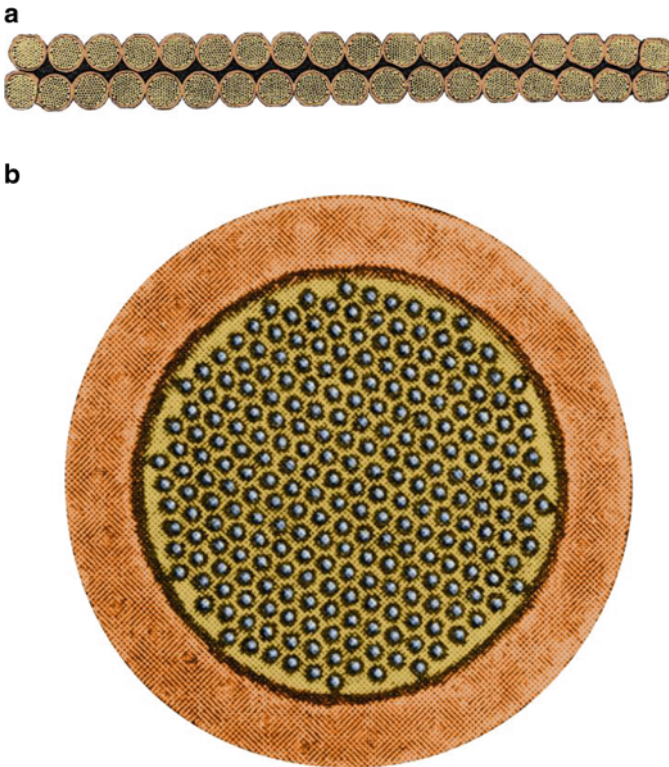
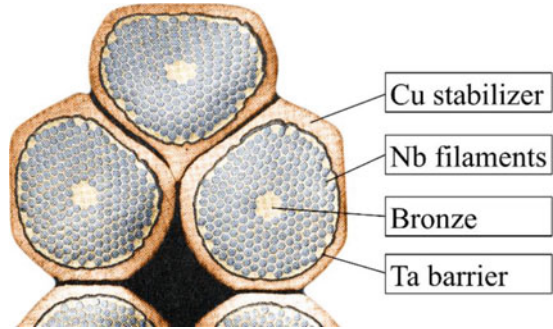


Fig. 4.3 Cross-section of: (a) outer layer cable; and (b) strand. (Courtesy of Vacuumschmelze GmbH, Germany)

extracted from the cables) and applying a reduction of 2% to take into account the expected degradation in cabling and a further 3% reduction due to degradation in bending around a 5 mm radius. The strand measurements were performed at the Vienna Technical University, Austria. These data showed that the magnet design parameters could be achieved with bronze route Nb₃Sn cables.

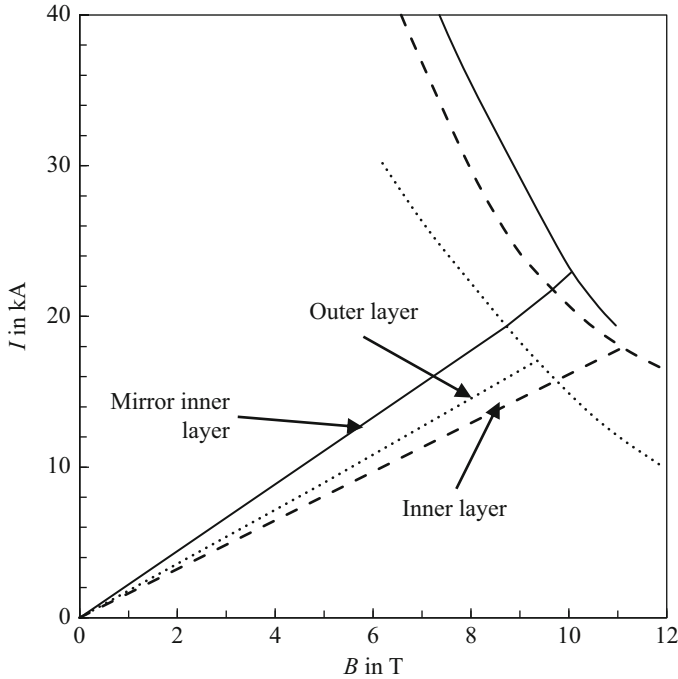


Fig. 4.4 Cable I_c vs. B dependence and computed coil load lines

Considering the limits in current density of the bronze route cables and the difficulty encountered in winding due to their stiffness, CERN with the University of Twente, Netherlands, had promoted the use of the innovative powder-in-tube (PIT) conductor under development by the Energy Research Centre of the Netherlands (ECN) (Hornsveld et al. 1988).

For this purpose, CERN ordered from ECN a small quantity of a pilot production of this conductor. A micrograph of a reacted filament is shown in Fig. 4.5, with voids seen in the core. The critical currents reported in Table 4.2 result from measurements performed at the University of Twente using a superconducting transformer (ten Kate et al. 1989). These high critical currents showed the potential of PIT conductors for the construction of high-field magnets. For particle accelerator magnets, however, considerable development was needed to reduce the filament diameter.

4.5 Magnetic and Mechanical Design

4.5.1 Magnetic Design

The conductors are arranged around the aperture in blocks separated by copper wedges to approximate the cos-theta current distribution. There are four blocks of

Fig. 4.5 Detail of a hexagon in the ECN conductor. (Modified from ten Kate et al. 1989)

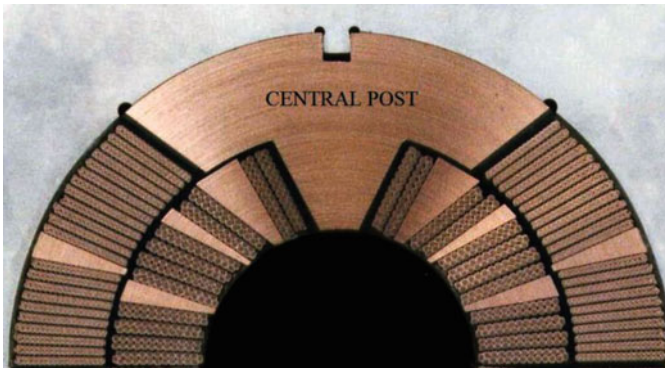
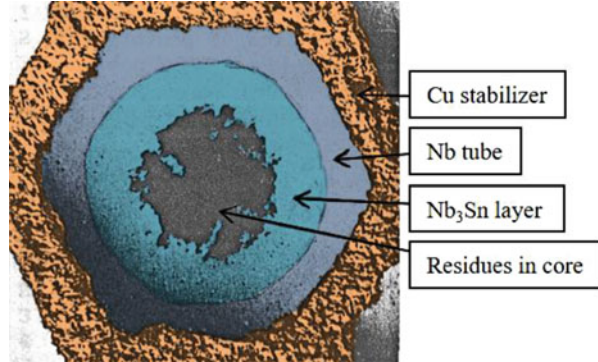


Fig. 4.6 Coil cross-section model. (Courtesy of ELIN, Austria)

conductors in the inner layer and two in the outer. The electromagnetic design started with an analytical approach in two dimensions (Perin 1973, 1995), taking into account the presence of a circular iron screen considered as an equipotential surface ($\mu = \infty$). The coil was subdivided into a number of small circular sectors of uniform current density, and their contribution to the field added up by means of a simple computer program. In this case, the coil cross-section, shown in Fig. 4.6, was determined to eliminate the first higher order multipoles.

The real iron with its variable permeability was then taken into account, using the MARE (Perin and van der Meer 1967) and POISSON (Halbach and Holsinger 1972) programs, in order to optimize yoke thickness, yoke–coil distance and yoke shape. At intermediate fields of about 7 T the computed $\Delta B/B_0$ was within 1×10^{-4} at $R_{\text{ref}} = 10$ mm.

The coil end shapes follow the constant perimeter configuration designed by ELIN using a program based on the Biot–Savart law. The conductor blocks are separated by insulated bronze spacers. The ends of the coil, for a dummy coil made from Cu–Ni cable, are shown in Fig. 4.7. This coil was used to practice coil winding and to test the entire manufacturing process, without wasting superconductors. The Cu–Ni cables had mechanical properties similar to the bronze route cables.

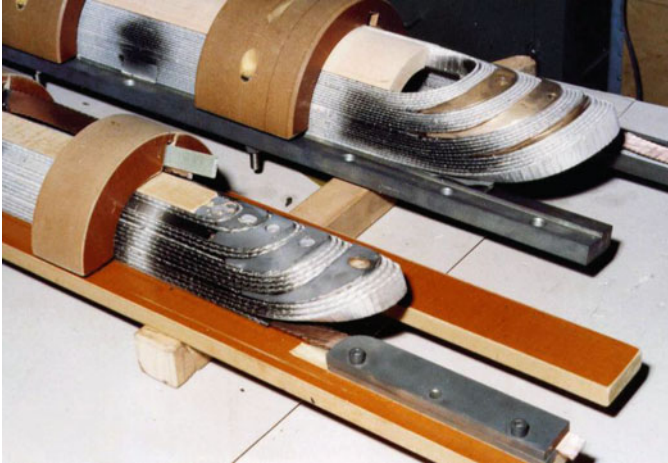


Fig. 4.7 View of the ends of inner and outer coil layers after reaction (Cu-Ni dummy). (Courtesy of ELIN, Austria)

4.5.2 Mechanical Design

A hybrid structure was chosen for retaining the Lorentz forces and providing the necessary compressive pre-stress on the coils (Perin 1986). This was known as a hybrid structure, as it produces a moderate compression at room temperature, to avoid creep of the coil materials, and the higher pre-stress required only under cold conditions. In addition, it greatly reduces the deformation of the coil–collar assembly when the magnet is powered.

The yoke dimension is chosen such that a ~ 0.5 mm gap between the yoke halves is maintained at room temperature. This gap closes between 150 K and 100 K during cool-down depending on the precise dimensions of the collars and yoke. The outer cylinder is shrink-fitted. Figure 4.1 provides an overview of the parts of the structure.

The ANSYS software program (Swanson Analysis System, USA) was used for the structural analysis for which the Young’s moduli E of the windings had been determined by measurements on reacted and impregnated cable stacks. Measurements up to 100 MPa pressure were performed in azimuthal and radial directions by pressing cable stacks in ad hoc made fixtures. Behavior close to linear was found above 40 MPa. The azimuthal E between 50 MPa and 80 MPa was about 19 GPa for the inner layer cable stacks and about 20 GPa for the outer layer. The radial E , almost equal for the inner and outer layer cable stacks, was about 24 GPa. The computed stresses at the pole and mid-plane of the coil at magnet assembly, cool-down and powering are reported in Fig. 4.8.

Results of measurements on Nb_3Sn strands and cables, available when the magnet was built, indicated a strong degradation of current density under transverse compression. For this reason, the pre-compression on the coil was limited to the minimum level to maintain contact at the interface with the central post in all operating conditions. Only 2 years later, new measurements made on assemblies

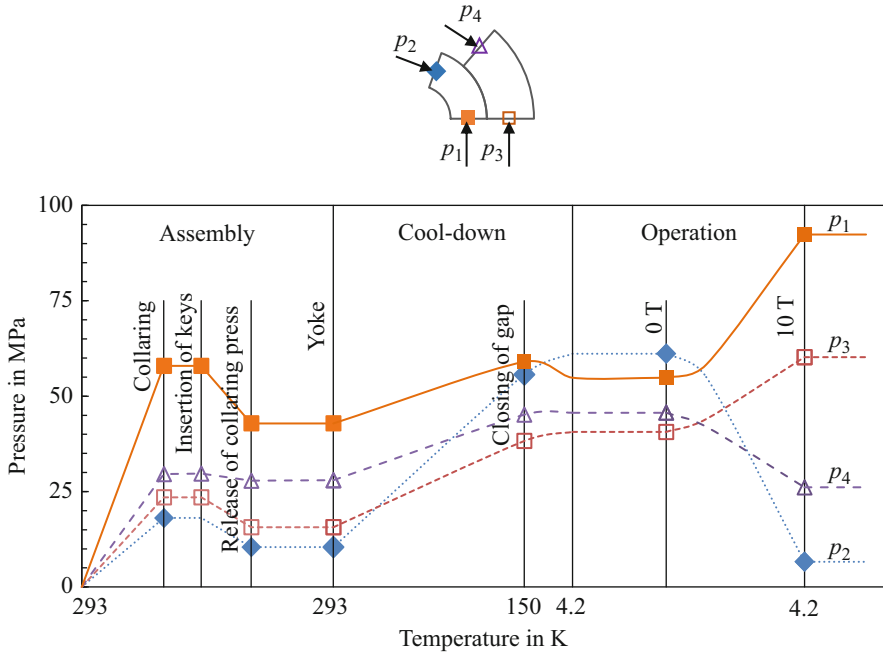


Fig. 4.8 Computed coil stresses at assembly, cool-down, and at 10 T bore field. (Courtesy of F. Zerobin)

of samples of the magnet cables reacted and epoxy-resin impregnated as in the magnet, showed much smaller reversible degradation (Bona et al. 1991): at $B = 10$ T less than 2% and about 4% under transverse compressions of 100 MPa and 150 MPa, respectively; at $B = 11.5$ T, 4% and 6% under the abovementioned compressions. This would have allowed a higher coil pre-compression of up to 150 MPa, which was the testing limit.

The axial Lorentz forces are taken at the coil ends by thick stainless-steel plates bolted to eight tie-rods passing through holes in the yoke.

4.6 Coil Manufacture and Magnet Assembly

The main components of a coil layer are:

- A central post, made of copper;
- Superconducting cables and their insulation;
- Longitudinal copper wedges;
- End spacers made of bronze.

A precise winding machine (Fig. 4.9) and sophisticated tooling were designed and built by ELIN, to shape the conductors and hold them in place during winding

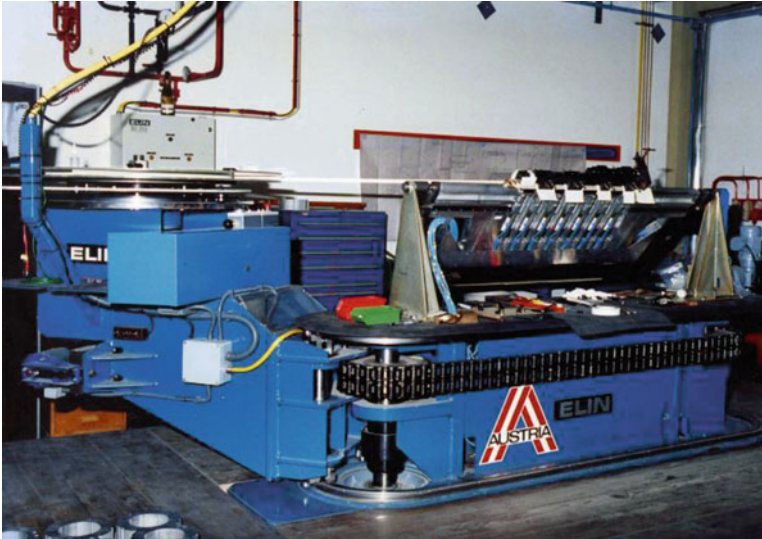


Fig. 4.9 Coil winding machine. (Courtesy of ELIN, Austria)

and the subsequent fabrication phases, since the bronze content made the conductors stiff and springy. This stiff and springy conductor required robust tools capable of applying large forces. No separate heat treatment mold was used, and therefore a part of the tooling used during winding had to be able to withstand the high temperature during reaction heat treatment for several hours. Stainless steel was the material generally used for various tooling.

The inter-turn insulation was made of half-overlapped 0.12 mm thick, 15 mm wide mica-glass tape (Cablosam® 366.21–10, Von Roll Isolawerke, Switzerland). This tape is composed of mica paper backed on one side by woven glass, and is entirely pre-impregnated with a flexible silicon elastomer. To ensure sufficient mechanical stability of the tiny mica flakes after firing of the organic elastomer, the tape was wound with the mica placed on the cable side, so that the external glass fiber (the mechanically stronger component) would maintain them in place and compress them against the cable. The same type of insulation tape was employed for the central post, the copper wedges, and the spacers at the coil ends.

The insulated wedges and end spacers were inserted during winding at the foreseen places. The end spacers were manufactured by casting and milling from bronze. The rough shape was obtained by casting. The final profile was made by inclining the milling cutter of a pre-determined angle and synchronically controlling the advance and rotation of the piece. Edges and corners were carefully rounded off to safeguard the insulation. An improvement of the insulation was tried by flame-spraying alumina, Al_2O_3 , but mica-glass tape was absolutely needed.

The winding of a coil layer is shown in Fig. 4.10. The insulated cables were wound under a tension of 500 N for the inner layer and about 300 N for the outer layer. After winding, each single-layer coil with its clamping and confining fixtures



Fig. 4.10 Winding a coil layer. (Courtesy of ELIN, Austria)

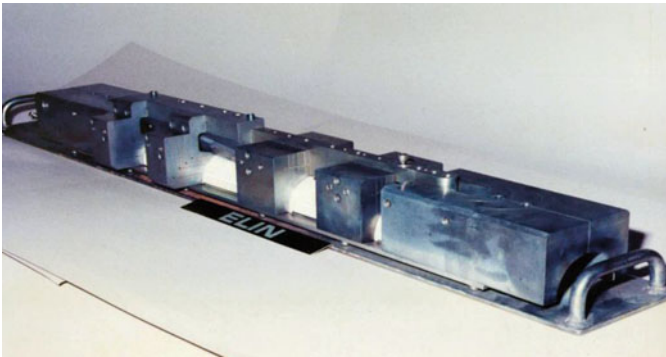


Fig. 4.11 A coil layer ready for reaction clamped by stainless-steel tooling blocks. (Courtesy of ELIN, Austria)

(Fig. 4.11) was placed in the reaction oven where the following operations were carried out: (1) evacuation at room temperature; (2) heating up to 600 °C in an argon atmosphere; (3) firing at 600 °C with dry air circulation for about half an hour in order to eliminate the organic component of the insulation; (4) evacuation; (5) heat treatment at 675 °C under flowing argon for about 140 h; (6) slow cool-down to room temperature under an argon atmosphere. The end view of a reacted coil inner layer is shown in Fig. 4.12.

After reaction, an inter-layer insulation sheet (Nomex®, DuPont, USA) was placed around the inner layer, the two coil layers were assembled, and the internal Nb₃Sn–Nb₃Sn splice between the inner and outer layers was made. The making of the splice, placed in the straight part of the coil, can be described as follows: during winding, the first turn of the inner layer is bent (the jump) to reach the level of the outer layer where it continues straight for about 250 mm (about two transposition lengths). The corresponding part of the outer layer cable first turn, also about

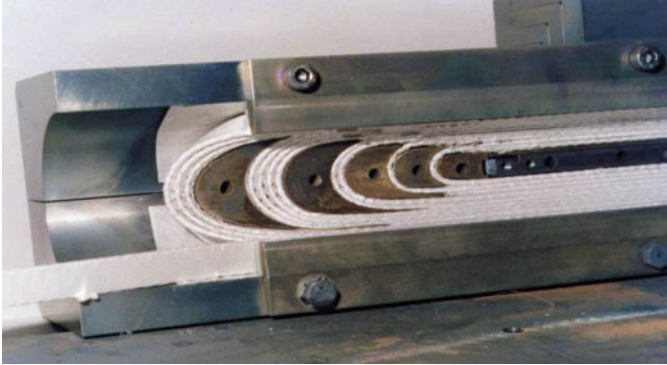


Fig. 4.12 End view of a reacted coil inner layer. (Courtesy of ELIN, Austria)

250 mm long, remains straight in its normal place. The soldering of the two corresponding parts is made by inserting between them a $\text{Pb}_{60}\text{Sn}_{40}$ foil, and then performing a pressing and heating operation. Two voltage taps are then soldered to the splice. For additional stability, the splice is then inserted and soldered in a U-shaped copper piece, which is insulated and lodged in a slot in the central post.

After placing the central post, the $\text{Nb}_3\text{Sn-Nb-Ti}$ splices of the coil terminals were also made using $\text{Pb}_{60}\text{Sn}_{40}$ solder. The coil-to-ground insulation (Nomex®) was wrapped around the coil, which was then placed in the impregnation mold, whose closing plate was tightened by bolts with a force of 600 kN in order to apply a tangential compression of about 10 MPa to the windings.

After evacuation, impregnation with epoxy resin and curing were performed with a similar resin and procedure that had been used in the CERN ISR superconducting quadrupoles (Billan et al. 1976): Ciba-Geigy, Switzerland resin system composed of Araldite MY745 (100 pbw) epoxy, HY905 hardener (100 pbw), and DY072 (1 pbw) and DY073 (0.2 pbw) accelerators. The impregnation was performed for 8 h at 90 °C and a curing cycle for 24 h at 120 °C.

After impregnation, the coil was extracted from the mold, cleaned of resin and demolding agent residues, and replaced into the mold to measure its elastic modulus. Measurements were made in the central part of the coil over 100 mm, paying attention not to introduce shear. After some pressing cycles to verify the reproducibility of force vs. displacement behavior, the E modulus was measured at pressures of around 50 MPa: the result for the coil azimuthal E modulus was about 28 GPa. This value was in relatively good agreement with the E measured on cable stacks (see Sect. 4.5.2). This result was used to determine the thickness of the shims inserted between the coils in the magnet median plane to obtain the pre-stress required at collaring.

The two coils were then assembled, and the collars were placed around them. After some pressing cycles to settle the assembly, the collars were pressed to the prescribed force and the locking keys inserted.

The yoke halves were then mounted with a slight compression, sufficient to guarantee integrity of the assembly during handling, and provisionally kept in place with belts. The stiff end plates were fixed to the tie rods. Finally, the outer aluminum alloy cylinder was shrink-fitted by warming it up to 200–250 °C. An insulating plate to support the external connections was fixed to the magnet end plates. The two coils were then soldered together with two Nb-Ti cable terminals and the lead Nb-Ti cables were fixed to their support.

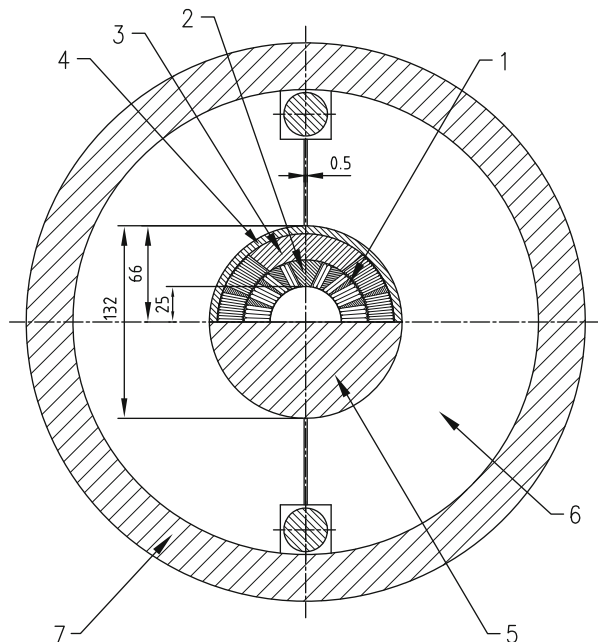
4.7 Mirror Coil Test Facility

A 1 m long, 5 cm diameter half-bore mirror dipole was built at ELIN to test single coils. Its cross-section is shown in Fig. 4.13. In the mirror dipole, one coil is replaced by an iron insert. In this set-up no collars were used: the necessary pre-stress on the coil is provided by the yoke halves surrounded by the aluminum shrinking cylinder.

4.8 Tests and Performance

The magnet prepared for installation in a Dewar is shown in Fig. 4.14. At various steps of magnet construction, voltage taps were placed: at the coil inter-layer splices, at the coil Nb₃Sn/Nb-Ti terminal splices, and at the magnet leads. All voltage taps

Fig. 4.13 Simplified cross-section of the Mirror Test Facility: 1 – coil; 2, 3 – central post parts; 4 – copper shield; 5 – iron mirror; 6 – iron yoke; 7 – shrinking cylinder



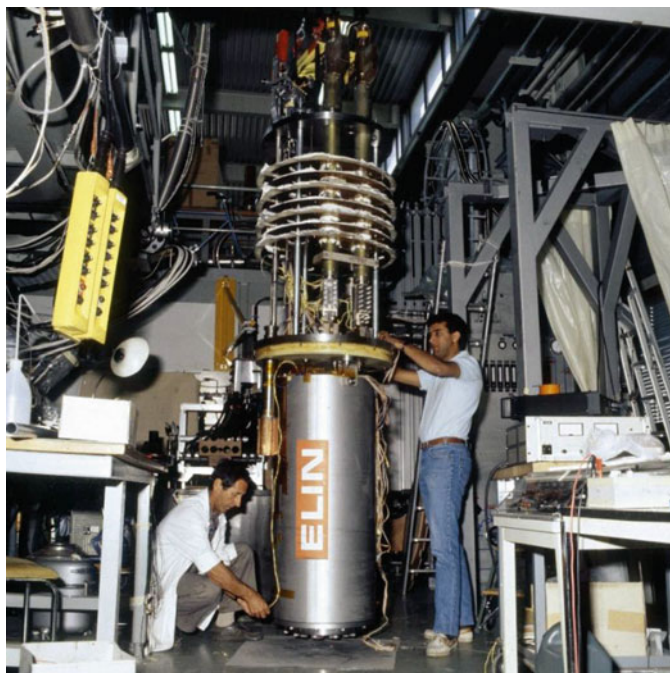


Fig. 4.14 The magnet ready to be inserted into a vertical cryostat for tests. (Courtesy of CERN)

were doubled for redundancy, so in total 12 voltage taps were installed. An elaborate protection system, with heaters for rapidly quenching the entire magnet, was not necessary for this short magnet and, therefore, not installed. Of course, for longer magnets such a system would be mandatory.

In this short model magnet, protection was ensured by two resistors inserted in the circuit. One resistor was placed across the magnet leads inside the cryostat, to provide protection in case one or both cryogenic current leads failed. The second resistor was placed outside the cryostat and was normally short-circuited by a circuit breaker. When a quench was detected (by comparing voltages across the two coils), the circuit breaker was opened, thus forcing the magnet current through the two resistors.

An early coil, mounted in the Mirror Coil Test Facility, had been tested in February 1989. It reached a central field of 10.2 T at 17,430 A, 4.3 K, after eight quenches (Fig. 4.15). The magnetic field was measured by means of a Hall plate magnetometer. After full thermal cycle, the same field was attained without retraining. When tested at 1.9 K the quench field was the same, an indication that the mechanical limit was reached. All quenches started in the inner layer of the coil.

The full magnet was tested in June 1989. It reached a central bore field of 9.5 T at a current of 15,600 A at 4.3 K, corresponding to about 10.05 T in a turn of the inner layer. Thermal cycling to room temperature did not affect the field level and negligible retraining occurred (Fig. 4.16). As in the mirror configuration, all

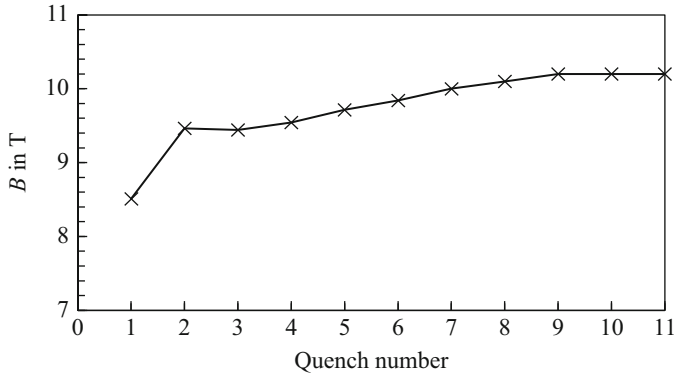


Fig. 4.15 Quench history of the mirror (half-dipole) at 4.3 K

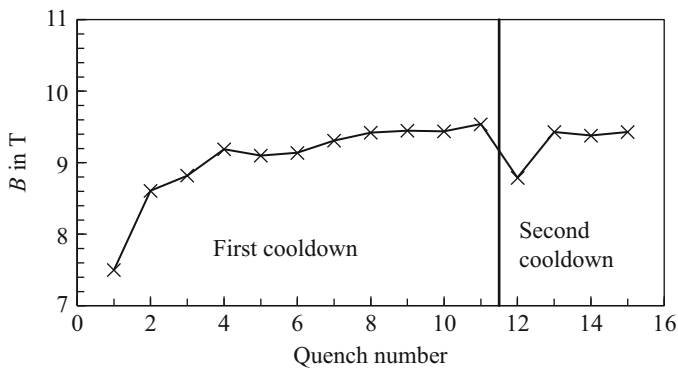


Fig. 4.16 Quench history of full dipole at 4.3 K

quenches started in the inner layer of the coils. The field attained in the dipole model was slightly lower than in the mirror configuration due to the lower Nb₃Sn content in the dipole inner-layer cable and the larger distance to the iron yoke.

4.9 Coil with Powder-in-Tube Cables

Upon delivery of the prototype cable lengths, a coil was manufactured by ELIN and mounted in the Mirror Coil Test Facility. Its construction followed the same procedure as the previous bronze route coils. It was tested in December 1991. The central field reached at the first quench was 7.43 T at a current of 11,270 A at 4.3 K, a remarkable result for a first experimental production of a novel conductor. More than 20 excitations were made. At small ramp rates up to 100 A/s all quenches happened at the same field level, about 7.4 T. A possible explanation could be that they were

caused by a localized defect in a conductor. Higher ramp rates affected the quenching field: 7.1 T at 200 A/s, 6 T at 250 A/s, and 5 T at 300 A/s. This could be due to the large Nb₃Sn filament size.

This was the last construction activity at that time at CERN on the Nb₃Sn option, as all CERN resources had to be concentrated on the Nb-Ti line. In Europe activity on Nb₃Sn magnets continued, with CERN's involvement, by a collaboration with the Netherlands Institute for Nuclear & High Energy Physics (NIKHEF), the Netherlands Foundation for Fundamental Research on Matter (FOM) and the University of Twente. This culminated in the successful construction of the Model Single of the University of Twente (MSUT) dipole model, which was tested at CERN in 1995, reaching 11.03 T at 4.4 K at its first quench.

4.10 Conclusion

In 1989 the CERN-ELIN model magnet made a real breakthrough in accelerator magnet technology. A moment of celebration of this success is shown in Fig. 4.17. It was the first successful dipole of particle accelerator type made with Nb₃Sn superconductor. It reached record field levels of 9.5 T in the full dipole and 10.2 T in the magnetic mirror configuration. Its design and fabrication were in an industrial style, showing that the Nb₃Sn option was a realistic one for attaining field levels not accessible to Nb-Ti. Considerable technological advancement was achieved, in particular concerning the electrical insulation of the cables, the coil winding, and the reaction process. The manufacturing of the coil was, however, complicated and delicate, requiring maximum attention at all steps.

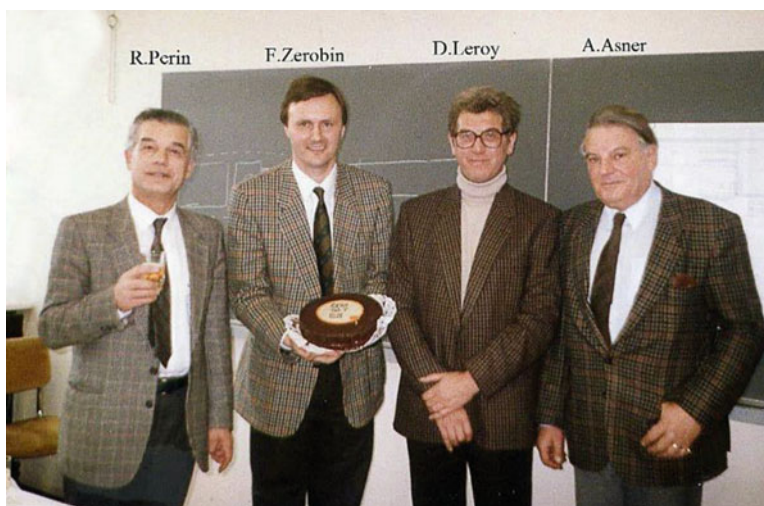


Fig. 4.17 Project leaders congratulate the team for the successful magnet test (17 June 1989)

It was recognized that important improvements were necessary to obtain better performing and less stiff conductors. The development of processes other than the bronze route such as jellyroll and PIT, still in their initial phases, had to be strongly supported because they promised higher current density and easier winding. One key challenge for PIT process development for use in particle accelerators was towards smaller filaments.

The cable insulation also needed great improvements in mechanical strength, flexibility, and resistance to high temperatures. At that time there was a consensus that insulation materials other than mica and glass should be investigated, for instance ceramics. These improvements on the basic materials, superconductors, and insulation, would lead to safer and more economical coil fabrication.

In 1991 CERN decided to adopt Nb-Ti for the LHC magnets, and consequently all CERN resources had to be concentrated on developing this technology. This decision was taken after thorough discussions at all levels. It was based on the following main arguments:

- The technology of Nb₃Sn superconductors was still in an experimental stage, while Nb-Ti was an industrial product manufactured and commercialized at market prices by several companies.
- Only one Nb₃Sn accelerator type short magnet and none of the length required for the LHC (10 m or more) had successfully been built.
- The cost of Nb₃Sn magnets was estimated to exceed by far the foreseen budget.
- Industrialization of superfluid cryogenics was deemed easier to achieve, less expensive, and less risky than that of Nb₃Sn magnets.

References

- Asner A, Perin R, Wenger S et al (1990) First Nb₃Sn, 1 m long superconducting dipole model magnets for LHC break the 10 Tesla field threshold. In: Sekiguchi T, Shimamoto S (eds) Proceedings 11th international conference on magnet technology, Tsukuba, 28 Aug–1 Sep 1989, vol 1. Springer, Dordrecht, pp 36–41, CERN LHC Note 105, Aug 1989
- Billan J, Perin R, Resegotti L et al (1976) Construction of a prototype superconducting quadrupole magnet for a high-luminosity insertion at the CERN intersecting storage rings. CERN Yellow Report 76–16, CERN, Geneva
- Bona M, Jakob B, Pasztor G et al (1991) Reduced sensitivity of Nb₃Sn epoxy-impregnated cable to transverse stress. *Cryogenics* 31(5):390–391; CERN LHC Note 141, Apr 1991. [https://doi.org/10.1016/0011-2275\(91\)90117-F](https://doi.org/10.1016/0011-2275(91)90117-F)
- Haebel EU, Wittgenstein F (1971) Big European Bubble Chamber (BEBC) magnet progress report. In: Derrick M (ed) Proceedings international conference on bubble chamber technology, June 1970, vol 2. Argonne National Laboratory, Argonne, pp 1126–1149
- Hagedorn D, Leroy D, Perin R (1985) Towards the development of high field superconducting magnets for a hadron collider in the LEP tunnel. In: Marinucci C, Weymuth P (eds) Proceedings of the 9th international conference on magnet technology, Swiss Institute for Nuclear Research (SIN), Villigen, pp 86–91, Zurich, 9–13 Sep 1985; CERN LHC Note 31, Aug 1985
- Halbach K, Holsinger R (1972) Poisson user manual. Technical Report, Lawrence Berkeley Laboratory, Berkeley

- Hornsveld EM, Elen JD, Van Beijnen CAM et al (1988) Development of ECN-type niobium-tin wire towards smaller filament size. *Adv Cryo Eng* 34:493–498
- Morpurgo M (1970) The design of the superconducting magnet for the OMEGA project. *Particle Accelerators* 1:255–263. <https://cds.cern.ch/record/350951/>
- Perin R (1973) Calculation of magnetic field in a cylindrical geometry produced by sector or layer windings. Internal note CERN ISR-MA/RP/cb, 15 Nov 1973. CERN, Geneva
- Perin R (1986) Magnet research and development for the CERN Large Hadron Collider. In: Dahl PF (ed) *Proceedings ICFA workshop on superconducting magnets and cryogenics*, Brookhaven National Laboratory, Upton, NY, 12–16 May 1986, BNL 52006 pp 25–33; CERN LHC Note 41, CERN SPS/86–9 EMA
- Perin R (1990) Superconducting magnets for the LHC: a report of CERN’s collaboration with industry, vol 21. CERN, *Europhysics News*, Geneva, pp 90–92
- Perin R (1995) Field, forces and mechanics of superconducting magnets, In: *Proceedings CAS superconductivity in particle accelerators*, 14–24 May 1995, Hamburg. CERN, Geneva pp 71–92 CERN Yellow Report 96–3
- Perin R, Van Der Meer S (1967) The program MARE for the design of two-dimensional static magnetic fields. CERN Yellow Report 67–7
- Perin R, Leroy D, Spigo G (1989) The first industry made model magnet for the CERN Large Hadron Collider. *IEEE Trans Magn* 25(2):1632–1635. <https://doi.org/10.1109/20.92612>. CERN LHC Note 83 Aug 1988
- Ten Kate HHJ, Ten Haken B, Wessel S (1989) Critical current measurements of prototype cables for the CERN LHC up to 50 kA and between 7 and 13 Tesla using a superconducting transformer circuit. In: Sekiguchi T, Shimamoto S (eds) *11th international conference on magnet technology (MT-11)*, Tsukuba, 28 Aug–1 Sep 1989. Springer, Dordrecht, pp 60–65
- Wenger S, Zerobin F, Asner A (1989) Towards a 1 m long high field Nb₃Sn dipole magnet of the ELIN-CERN collaboration for the LHC-project-development and technological aspects. *IEEE Trans Magn* 25(2):1636–1639. <https://doi.org/10.1109/20.92613>. CERN LHC Note 82 Aug 1988
- Wilson RR (1978) The Tevatron. FERMILAB-TM-0763
- Wolff S (1988) Superconducting HERA magnets. *IEEE Trans Magn* 24(2):719–722. <https://doi.org/10.1109/20.11326>

Open Access This chapter is licensed under the terms of the Creative Commons Attribution 4.0 International License (<http://creativecommons.org/licenses/by/4.0/>), which permits use, sharing, adaptation, distribution and reproduction in any medium or format, as long as you give appropriate credit to the original author(s) and the source, provide a link to the Creative Commons licence and indicate if changes were made.

The images or other third party material in this chapter are included in the chapter’s Creative Commons licence, unless indicated otherwise in a credit line to the material. If material is not included in the chapter’s Creative Commons licence and your intended use is not permitted by statutory regulation or exceeds the permitted use, you will need to obtain permission directly from the copyright holder.

